JOURNAL OF CATALYSIS 113, 144–163 (1988)

Methane Utilization by Oxidative Coupling

I. A Study of Reactions in the Gas Phase during the Cofeeding of Methane and Oxygen

GERALD S. LANE AND EDUARDO E. WOLF[1]

Department of Chemical Engineering, University of Notre Dame, Notre Dame, Indiana 46556

Received October 8, 1987; revised April 20, 1988

The oxidative coupling of methane has been investigated in the absence of catalysts by cofeeding methane and oxygen. A survey on the effects of varying several operating conditions shows that under certain conditions significant gas-phase oxidative coupling can occur in the absence of catalysts. The reaction products were C_2H_6, C_2H_4, C_3H_8, C_3H_6, CO (the main oxidation product), CO_2, H_2, H_2O, and traces of HCHO and C_4 and C_5 hydrocarbons when conversions were high. The general trend dictated by the gas-phase kinetics is that the hydrocarbon product selectivity falls as the conversion increases. Specifically, at methane conversions of 2%, the hydrocarbon product selectivity was around 65%, but when methane conversions were increased to 32%, the hydrocarbon selectivity decreased to 29%. The apparent activation energy for methane conversion in the gas phase was found to be around 55 kcal/mole which is similar to that reported for the gas-phase reaction of methane and molecular oxygen forming methyl and hydroperoxy radicals. Several gas-phase results have been presented for comparative purposes with catalytic oxidative coupling studies. A reaction pathway for the gas-phase oxidative coupling network has been considered and compared to proposed catalytic reaction pathways. The implications that the observed results might have on catalytic oxidative coupling of methane have also been considered. © 1988 Academic Press, Inc.

INTRODUCTION

In recent years, there has been a renewed research effort to find a viable means of converting methane into more valuable chemicals. Several avenues have been investigated in attempting to convert methane to transportable liquid products or to more valuable chemicals such as ethylene. The difficulty in converting methane is its high stability relative to any product to which it might be converted. The high dissociation energy of the first C–H bond is around 104 kcal/mole (435 kJ/mole) (*1*); hence, the rate-limiting step in methane conversion is the abstraction of the first hydrogen from methane. High temperatures are required to abstract hydrogen from methane and are predicted by thermodynamics as demonstrated by Keller and Bhasin (*2*) and Pitchai and Klier (*3*). Reports on the pyrolysis of methane (*4, 5*) have indicated that a combination of short residence times and high temperatures (>1200°C) is required to achieve high selectivities of acetylene and hydrogen. A second route for the conversion of methane, used industrially, is the production of synthesis gas by catalytic steam reforming of methane and has been reviewed by Van Hook (*6*) and Bartholomew (*7*).

An alternative route for methane conversion is oxidative coupling. As pointed out by Pitchai and Klier (*3*) and Scurrell (*8*), the positive free energies encountered in trying to dehydrogenate methane are overcome in an oxygen environment as both free energy changes and heats of reaction become

[1] To whom correspondence should be addressed.

0021-9517/88 $3.00
Copyright © 1988 by Academic Press, Inc.
All rights of reproduction in any form reserved.

favorable with the formation of water instead of hydrogen. In oxidative coupling, both molecular oxygen and nitrous oxide have been used as oxygen sources to induce favorable thermodynamics. The use of methane and nitrous oxide over a variety of catalysts has been demonstrated to be somewhat successful (*9–16*); however, economic considerations rule out the use of nitrous oxide as a coreactant.

Currently, the most active area of methane utilization research is the use of methane and oxygen. Several approaches for converting methane in oxygen-containing environments are being investigated. One approach is the conversion of methane directly to oxygenates like methanol and formaldehyde and was recently been reviewed by Pitchai and Klier (*3*) and by Gesser *et al.* (*17*). A second approach is the oxidative coupling of methane to ethane and ethylene using metal oxides as catalysts. The selective production of ethylene from methane has tremendous advantages over the currently used precursors for ethylene production. Significant research interest in this area was generated after Keller and Bhasin reported the conversion of methane to ethane and ethylene using a variety of metal oxides (*2*).

Two different approaches have been used in the oxidative coupling of methane to higher hydrocarbons: a cyclic feeding operation and a cofeeding operation. The first approach follows the method used by Keller and Bhasin (*2*) in which methane and oxygen are cyclically fed to minimize the conversion of methane in the gas phase and to minimize sequential combustion of hydrocarbon products. This method involves fully oxidizing the catalyst, purging the oxygen, and flowing methane over the catalyst. After flowing methane, the reactor is purged, and the cycle is repeated. This approach has been used by several groups on a variety of metal oxide catalysts (*2, 18–21*) which are reported to undergo a Mars–van Krevelen-type mechanism (*22*) with the lattice oxygen participating in a redox cycle. The second route for the oxidative coupling of methane involves continuous cofeeding of methane and oxygen and has been reported by several groups (*23–47*) to give fairly high selectivities for a variety of catalysts and operating conditions. Table 1 summarizes some of the operating conditions reported for several oxidative coupling studies using the cofeeding of methane and oxygen. In both methods of feeding the reactants, a general consensus indicates that methyl radicals combine to form ethane which can be oxidatively or thermally dehydrogenated to ethylene. Depending on which catalyst is chosen, CO and CO_2 can be produced directly from methane, from C_2H_6 and C_2H_4, or from methyl radicals. In some catalytic studies, the conditions under which blank runs (without a catalyst) have been conducted ar not clearly specified; furthermore, some catalytic studies have often reported results under operating conditions different from those used for testing activity in the absence of a catalyst.

Due to the similarity of results obtained in our preliminary work with and without catalysts, it was deemed important to systematically study the degree of oxidative coupling of methane that can occur in the absence of catalysts. A variety of operating conditions was surveyed and many gave rise to the conversion of methane to higher hydrocarbons, H_2, CO, CO_2, and H_2O. All experiments in this study were performed using fuel-rich compositions to maximize oxidative coupling and to minimize complete combustion. In contrast to gas-phase combustion studies using oxygen-rich feeds and to catalytic oxidative coupling studies, this study provides evidence that under certain operating conditions molecular oxygen in the gas phase is capable of initiating the oxidative coupling reaction pathway. This report demonstrates the effects of various operating conditions on gas-phase conversions and product selectivities. Lumped kinetic values were also determined from the gas-phase oxidative coupling results, and a

TABLE 1

A Summary of Literature Conditions for the Cofeeding of Methane and Oxygen[a]

Reactor		Temperature (°C)	Mass catalyst (g)	Flow rates (cc/min)				CH_4/O_2[b]	D[c]	Reference
Material	Size (mm)			He	N_2	CH_4	O_2			
*[d]	8 o.d.	400–800	2.0	50.0	3.0	1.5	0.75	2.0	0.04	(23)
SS[e]	9 i.d.	550–700	0.035	50.0	40.0	100.0	10.0	10.0	0.55	(24)
Quartz	10 i.d.	700–800	1.0	0.0	344.0	56.2	6.4	8.75	0.15	(25)
Quartz	6 i.d.	740	0.05–0.10	0.0	9.2	28.0	2.8	10.0	0.77	(26)
Quartz	6 i.d.	650–750	0.05–0.10	0.0	9.2	28.0	2.8	10.0	0.77	(27
Quartz	14 i.d.	710	0.3 (ml)	0.0	16.0	20.0	4.0	5.0	0.60	(28)
Quartz	23 o.d.	550–770	0.5–4.0	28.0	0.0	21.0	1.0	21.0	0.44	(29)
Quartz	23 o.d.	600–800	4.0	20.7	0.0	19.1	10.2	1.9	0.59	(30)
*	8 o.d.	400–800	2.0	50.0	3.0	1.5	0.75	2.0	0.04	(31)
Quartz	*	600–800	*	0.0	16.6	20.8	4.2	5.0	0.60	(32)
Quartz	25 i.d.	525–725	1.0	23.0	0.0	1.8	0.56	3.3	0.10	(33)
*	*	625–700	0.8	47.0	0.0	5.5	2.7	2.1	0.15	(34)
*	*	600–800	2.0	24.6	0.0	17.2	8.2	2.0	0.51	(35)
*	8 o.d.	400–800	2.0	50.0	3.0	1.5	0.75	2.0	0.04	(36)
*	*	750	1.0	33.3	0.0	1.8	0.90	2.0	0.08	(39)
Alumina	11 i.d.	750	2.0	47.0	0.0	9.6	4.3	2.3	0.23	(40)
*	*	750	0.01–0.15	0.0	0.0	24.0	4.0	6.0	1.00	(41)
*	*	750	1.0	33.3	0.0	1.8	0.90	2.0	0.08	(42)
Quartz	20 i.d.	600–800	0.5	30.6	0.0	6.7	0.15	45.5	0.18	(44)
*	*	750	0.40	17.0	0.0	55.3	27.7	2.0	0.83	(46)
*	*	600–830	0.50	28.0	0.0	23.4	4.7	5.0	0.50	(47)

[a] In some reports, flow rates and temperatures were varied; this table summarizes the standard experimental conditions of each report. Some of the values in this table were determined by making some assumptions about the exact conditions when they were not specified by the authors.

[b] Mole ratio of methane-to-oxygen in the feed.

[c] Dilution ratio, $D = (P_{CH_4} + P_{O_2})/P_{TOTAL}$.

[d] *, Not enough information was provided by the author to determine this condition.

[e] SS, stainless steel.

possible reaction pathway is presented based on this information.

EXPERIMENTAL

A concern in the design of the experimental apparatus was the selection of a reactor whose walls would not contribute significantly to the overall conversion. After testing several reactors of various types, styles, and shapes, tubular flow reactors made of fused silica (referred to as quartz) with inside diameters of 0.95 cm and with heated lengths of 15 cm were selected for most of the experiments being reported. The reactor was operated in a single-pass mode and was heated resistively with a furnace designed and built to minimize the heated length and provide heat transfer in a reproducible manner. The temperature of the reactor was monitored both outside (at the reactor wall) and inside the reactor using K-type thermocouples shielded with quartz thermocouple wells. The inside quartz thermocouple well was centered along the length of the reactor and provided a measure of the temperature in the axial direction. Figure 1 represents a diagram of the reactor, thermocouple assembly, and furnace used in this study. The reactor temperature was kept constant by an Omega 2012 programmable temperature controller monitoring the inside temperature at the hottest location. The programmability provided a convenient, reproducible way of controlling the reactor temperature for each experiment. The axial temperature gradient within the reactor was periodically checked by moving the location of the reactor thermocouple. Over the 15-cm heated length, the middle 10 cm was always ±1% of the set point; however, end effects are significant as the inlet and exit of the reactor are

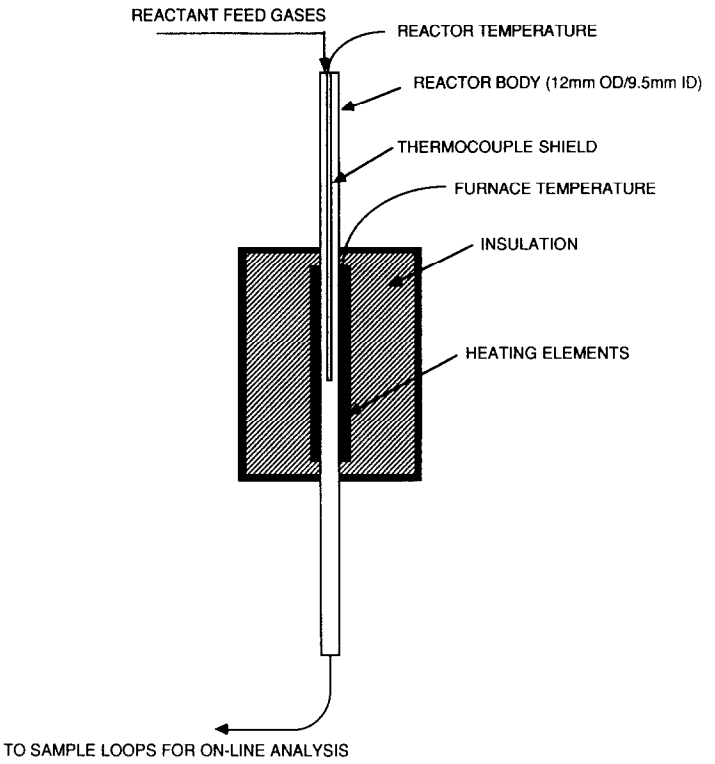

FIG. 1. Diagram of the reactor, thermocouple assembly, and furnace drawn approximately to scale.

uninsulated. The flow rate of each component in the feed was controlled and regulated by electronic mass flow controllers (Brooks Instrument Co.). Additional studies were performed in a $\frac{3}{8}$-in.-i.d. (0.95-cm) high-purity alumina (99.8%) tube from McDanel Refractories, Inc. with a heated length of 15 cm. A few comparative experiments were also carried out using a $\frac{1}{2}$-in.-o.d. (10.8-cm-i.d.) stainless-steel type 304 tube which had a 15-cm heated length. The same flow control system, furnace, and temperature controller used for the quartz reactor experiments were also used for the experiments with the alumina and stainless-steel reactors.

All results presented in this paper are for experiments in which methane and oxygen were cofed. Helium was chosen as an inert diluent to adjust the total pressure to 1 atm (1 atm = 101.3 kPa) because of its high thermal conductivity and because it did not interfere with the chromatographic output. The gases, used as delivered without purification, were ultrahigh-purity grades obtained from Union Carbide's Linde Specialty Gases Division and were of the following purities: CH_4 (99.97%), O_2 (99.99%), and He (99.999%).

Product analyses were performed by on-line gas chromatography (GC) using a thermal conductivity detector on a Carle GC (Model AGC 111) equipped with thermistors. Water was removed from the reaction products by a trap placed at the reactor exit to eliminate the presence of a broad water peak from the GC analysis. The major products were C_2H_6, C_2H_4, C_3H_8, C_3H_6, CO, CO_2, H_2, and H_2O. Two columns were operated in parallel to achieve sufficient separation of the products and reactants: a Carbosphere-packed column ($\frac{1}{8}$ in. × 6 ft) was used for the separation of hydrogen, oxygen, methane, carbon monoxide, and

carbon dioxide, and a HayeSep Q polymer-packed column ($\frac{1}{8}$ in. × 6 ft) was used for the separation of carbon dioxide, ethane, ethylene, propylene, and propane. Trace quantities of other hydrocarbons (C_4, C_5, and C_6 hydrocarbons) were analyzed using a Varian 1400 GC with a flame ionization detector and a Porapak Q column ($\frac{1}{8}$ in. × 20 ft). Feed and effluent compositions were calculated using external standards, and the closures on the carbon mass balances were within 5% and in most cases were within 2%; hydrogen and oxygen mass balances typically closed within 5% based on overall mass balances. Effluent flow rates were measured with a bubble meter at the exits of the GC sample loops to correct for the change in the number of moles due to reaction and condensation of products in the cold trap.

The operating conditions were varied over a range of conditions, within experimental constraints, to study the effects on methane conversion. Under any given set of flow conditions, the reactant and products were analyzed after reaching steady state in 50°C intervals over the temperature range from 600 to 800°C. The partial pressures of both methane and oxygen were varied, but care was taken to avoid the explosive limits. Although older reports are available on the explosive limits for methane–air mixtures (*48–51*), little has been published on the upper explosive limit (fuel-rich) for methane and oxygen mixtures at elevated temperatures. Since all experiments were conducted in the fuel-rich region, the conversion of oxygen always exceeded that of methane and shifted the reaction gases away from explosive compositions. The feed partial pressures of methane and oxygen were varied from 0.16 to 1.0 atm and from 0.0 to 0.33 atm, respectively, but the methane-to-oxygen feed mole ratio was never allowed to be less than 2. The effects of diluting the reactant stream with helium were studied by varying dilution ratios at constant residence times and constant methane-to-oxygen feed mole ratios. The dilution ratio, D, was defined as the partial pressure of methane and oxygen divided by the total pressure (1 atm). A typical set of operating conditions was a methane-to-oxygen mole ratio of 2 in the feed, a feed flow rate, Q, of 50 cc/min (measured at room temperature), a dilution ratio, D, of 0.7, and temperatures from 600 to 850°C.

The reactor was operated without any packing material, except for comparative experiments conducted with quartz wool and quartz chips placed in the heated zone of the reactor. The quartz chips were broken fragments of the same fused-silica material used for the reactor walls and had a surface area of approximately 0.01 m^2 which is about twice the area of the heated reactor walls. The bed porosity or void fraction of the reactor filled with the quartz chips was approximately 0.68.

RESULTS

The importance of gas-phase oxidative coupling of methane will be demonstrated under several different operating conditions and these results will be compared to those reported in catalytic studies. In all figures, the symbols depict experimental results, and the lines represent visual interpolations of these results, except in Figs. 7 and 8, where these interpolations were made by a multivariable linear fit.

In this paper, the following nomenclature has been used: (i) product selectivity has been defined as the amount of carbon converted to a given product divided by the total amount of carbon converted and has been expressed as a percentage; (ii) methane conversion, expressed as a percentage, was defined as one minus the amount of carbon in the products divided by the amount of methane fed; and (iii) oxygen conversion, expressed as a percentage, was defined as one minus the amount of oxygen detected in the effluent stream divided by the amount of oxygen fed.

(*a*) *Dilution effects.* A number of catalytic oxidative coupling of methane studies have used He, Ar, and N_2 as inert carrier gases to dilute the reactant stream. In this

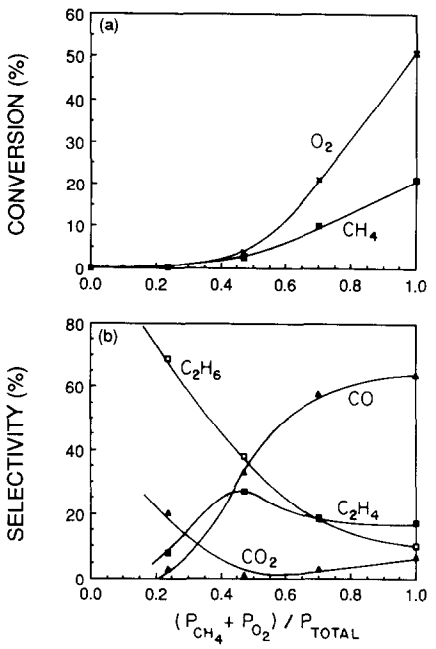

FIG. 2. The effect of the dilution ratio on methane and oxygen conversions and on product selectivities at 750°C in an empty quartz reactor with a feed mole ratio of methane-to-oxygen of 2 and with a total feed flow rate of 50 cc/min. (a) ×, represents oxygen conversion; ■, represents methane conversion. (b) □, represents ethane selectivity; ■, represents ethylene selectivity; △, represents CO selectivity; and ▲, represents CO_2 selectivity.

study, the effects of diluting the reactant stream were studied at constant residence times and constant mole ratios of methane-to-oxygen in the feed. The dilution ratio (D), defined as the partial pressure of methane and oxygen divided by the total pressure, represents the pressure fraction of the reactants in the feed. Figures 2a and 2b show the influence of varying the dilution ratio at 750°C for a methane-to-oxygen feed mole ratio of 2 and for a feed flow rate of 50 cc/min. Figure 2a shows that low conversions are obtained for D less than 0.4 and is consistent with literature results reported for empty reactors using diluted feeds which have concluded that gas-phase reaction or reactor wall effects were negligible under these conditions. However, for $D >$ 0.4, Fig. 2 shows that significant conversion and product selectivities can be attained under other conditions. In fact when no diluent is used, $D = 1$, methane conversions reached 21%, and hydrocarbon selectivities were around 30% at 750°C. Many of the experiments show trends in product selectivities and conversion similar to those depicted in Figs. 2a and 2b. As conversion increases, the product selectivity of ethane decreases; the CO product selectivity increases, and the conversion to CO_2 remains low for these conditions. The effect of a diluent at other temperatures showed similar trends, although at any given D, methane and oxygen conversions were lower for lower temperatures and likewise higher for temperatures greater than 750°C.

(*b*) *Residence time.* The bed length and contact time have been reported to have important roles in catalytic oxidative coupling of methane due to the secondary oxidation of the hydrocarbon products (*21, 40, 43, 46*). In this work, the influence of residence time was investigated in the absence of a catalyst by varying the volumetric feed flow rate. The volume of the reactor in which the gas-phase reactions take place is not known; thus instead of using residence time, the results are reported in terms of the inverse volumetric feed flow rate. Figure 3 displays conversion and product selectivity results from residence time studies at 650°C (Figs. 3a and 3b) and 750°C (Figs. 3c and 3d) using dilution ratios of 0.7 and methane-to-oxygen feed mole ratios of 2. It should be pointed out that each portion of Fig. 3 has a different scale on the ordinate axis. At both temperatures, conversions increase with increasing residence time (decreasing feed flow rate), but at 750°C the methane conversion levels out due to the high oxygen conversion. Many of the trends in product selectivity reflected in Figs. 3b and 3d are similar to those in Fig. 2b. When the residence time (or methane conversion) is increased, the conversion to CO increases coinciding with a decrease in ethane selectivity. In addition, at temperatures less than 675°C, the conversion to CO demonstrates

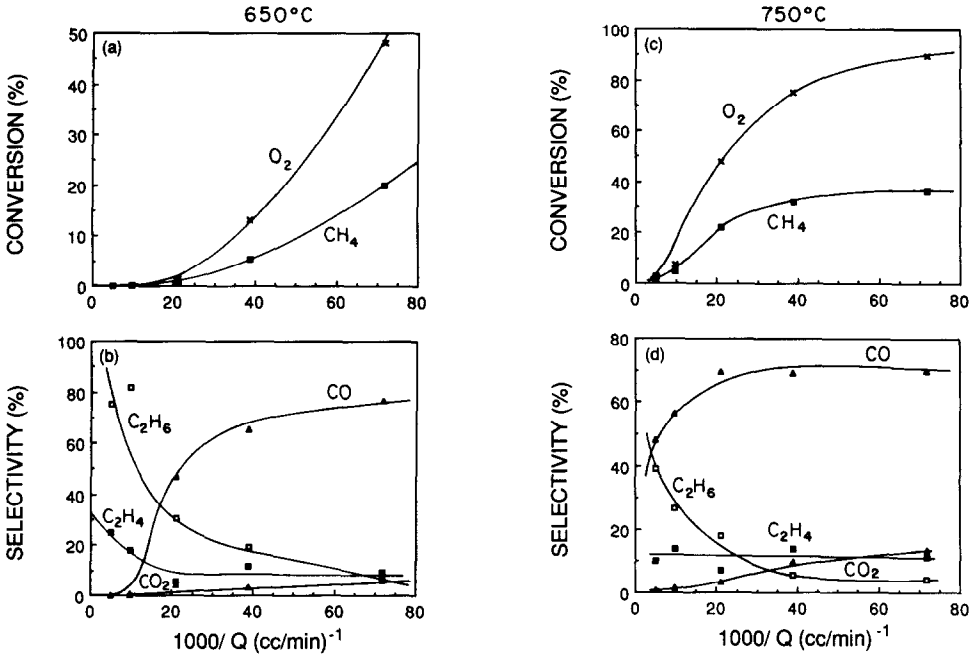

FIG. 3. The effect of residence time on methane and oxygen conversions and on product selectivities at 650 and 750°C in an empty quartz reactor with a feed mole ratio of methane-to-oxygen of 2 and with a dilution ratio of 0.7. (a and c) ×, represents oxygen conversion; ■, represents methane conversion. (b and d) □, represents ethane selectivity; ■, represents ethylene selectivity; △, represents CO selectivity; and ▲, represents CO_2 selectivity.

a light off-type behavior similar to that shown at 650°C in Fig. 3b. At short residence times the rate of CO production is very low, and the hydrocarbon selectivity is high; however, by increasing residence time or conversion, the rate of CO production increases rapidly.

(*c*) *Oxygen partial pressure.* Little attention has been given to the effect of the oxygen partial pressure in many of the catalytic oxidative coupling studies. Several catalytic studies, summarized in Table 1, have used conditions in which oxygen partial pressures were below 0.2 atm and have concluded that reaction rates were negligible in the gas phase. The results displayed in Figs. 4a and 4b show the influence of the oxygen partial pressure on methane and oxygen conversions and on product selectivities for experiments at 750°C with methane partial pressures of 0.66 atm and for total feed flow rates of 50 cc/min. At low oxygen partial pressures, $P_{O_2} < 0.2$ atm, the conversion of methane is less than 2%; however, gas-phase reaction rates become important if the oxygen partial pressure is greater than 0.2 atm. Product selectivities are strongly affected by oxygen partial pressure and show trends similar to those observed in previous figures. As conversion increases, the CO selectivity increases at the expense of ethane selectivity and displays an ignition-type behavior for $0.17 < P_{O_2} < 0.22$ atm or for a CH_4/O_2 feed mole ratio of about 3. At low oxygen partial pressures and low conversions, the selectivity to higher hydrocarbons exceeds 80%, whereas, at high oxygen partial pressures or low CH_4/O_2 mole ratios, the hydrocarbon product selectivity falls to around 30%.

(*d*) *Methane partial pressure.* Relatively little has been reported on the importance of the methane partial pressure or the methane-to-oxygen mole ratio in the catalytic

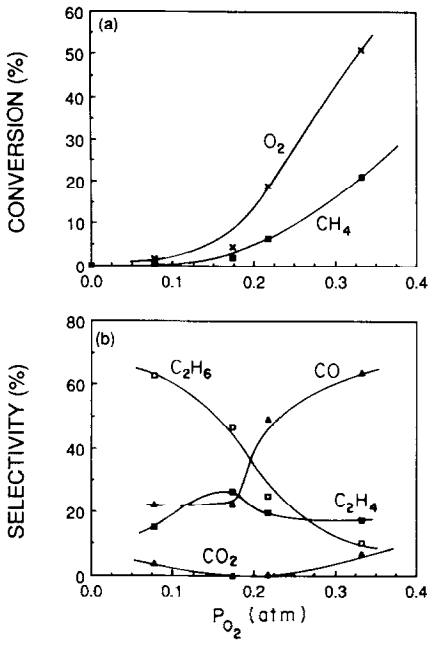

FIG. 4. The effect of oxygen partial pressure on methane and oxygen conversions and on product selectivities at 750°C in an empty quartz reactor with a total feed flow rate of 50 cc/min and a methane partial pressure of 0.66 atm. (a) ×, represents oxygen conversion; ■, represents methane conversion. (b) □, represents ethane selectivity; ■, represents ethylene selectivity; △, represents CO selectivity; and ▲, represents CO_2 selectivity.

oxidative coupling of methane. Figure 5 shows results on the influence of methane partial pressure for experiments with feed flow rates of 50 cc/min and temperatures of 800°C. During these experiments, the oxygen partial pressures were kept low (P_{O_2} = 0.08 atm) to allow a wide range of methane partial pressures to be tested without crossing into the region of explosive compositions. Since the oxygen partial pressure was low, methane and oxygen conversions are lower than those presented in previous figures. Consequently, the hydrocabon product selectivity remains greater than 60% for the range of methane partial pressures used. At these low conversions, both methane conversion and CO product selectivity slightly decreased as the methane partial pressure was increased (see Figs. 5a and 5b); whereas hydrocarbon selectivity was relatively insensitive to changes in the methane partial pressure.

When methane was fed without oxygen, no reaction was observed for temperatures less than 850°C, and this is consistent with studies on methane pyrolysis which have indicated that methane is converted at temperatures greater than 1000°C (*4, 5*). All oxidative coupling experiments in this study were conducted between 600 and 850°C and showed that methane conversion occurred in the presence of oxygen at temperatures much lower than those in the absence of oxygen. This indicates that some type of gas-phase oxygen species is required to activate methane at these lower temperatures.

(*e*) *Temperature effects.* Figure 6 displays the influence of temperature under

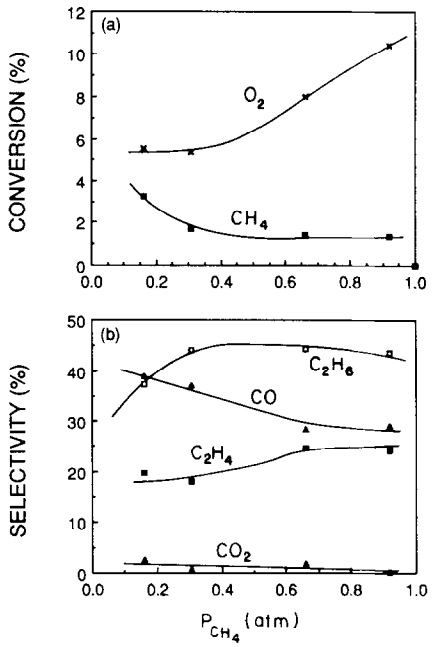

FIG. 5. The effect of methane partial pressure on methane and oxygen conversions and on product selectivities at 750°C in an empty quartz reactor with a total feed flow rate of 50 cc/min and an oxygen partial pressure of 0.08 atm. (a) ×, represents oxygen conversion; ■, represents methane conversion. (b) □, represents ethane selectivity; ■, represents ethylene selectivity; △, represents CO selectivity; and ▲, represents CO_2 selectivity.

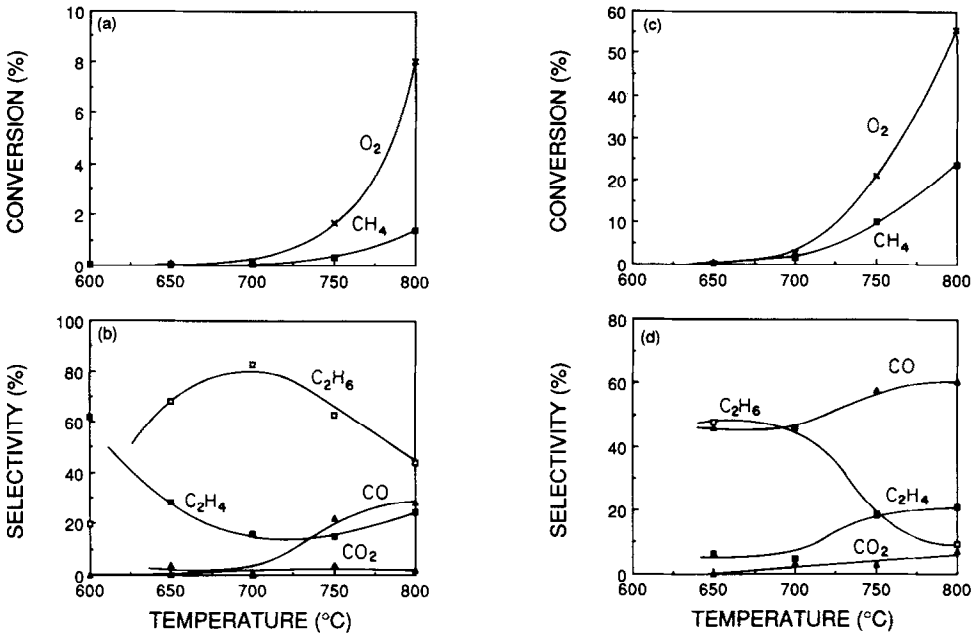

FIG. 6. A comparison of temperature effects on methane and oxygen conversions and on product selectivities in an empty quartz reactor with a total feed flow rate of 50 cc/min and under the following conditions. In a and b the methane partial pressure is 0.66 atm, the oxygen partial pressure is 0.08 atm, and the dilution ratio is 0.74. In c and d the methane partial pressure is 0.47 atm, the oxygen partial pressure is 0.23 atm, and the dilution ratio is 0.7. (a and c) ×, represents oxygen conversion; ■, represents methane conversion. (b and d) □, represents ethane selectivity; ■, represents ethylene selectivity; △, represents CO selectivity; and ▲, represents CO_2 selectivity.

different conditions. In addition, Fig. 3 compares the influence of residence time (or feed flow rate) at 650 and 750°C. Higher temperatures always resulted in higher conversions of methane and oxygen, but the product selectivity to higher hydrocarbons decreased as conversions increased. Figure 6 shows the effects of temperature for a dilution ratio, D, of about 0.7, a total feed flow rate of 50 cc/min, and oxygen partial pressures of 0.08 atm (Figs. 6a and 6b) and 0.23 atm (Figs. 6c and 6d). Although conversions were much lower for the low oxygen partial pressure (note that the ordinate axes have different scales), conversions were low for temperatures less than 700°C for both partial pressures and increased as temperature increased. The product selectivities for the two different partial pressures of oxygen (Figs. 6b and 6d) show different behavior as a function of temperature. While Fig. 6b shows ethane selectivity going through a maximum, Fig. 6d shows that ethane selectivity decreases while ethylene selectivity slightly increases suggesting that some of the ethylene is produced from the oxidative dehydrogenation of ethane.

(f) Reactor materials. As previously mentioned, a concern at the outset of this project was choosing an inert reactor wall material. Reaction tests and reports in the literature have indicated that stainless steel is sufficiently active to give significant conversion due to the walls of the reactor (*8*). Other studies have used quartz and alumina reactors and have reported no activity on the reactor walls under the conditions tested; however, Shtern has indicated that various treatments of quartz reactors can create surfaces that are active for methane oxidation (*52*). In this study in order to test

TABLE 2

A Comparison of Reactor Materials to Determine the Importance of Wall Effects

Reactor material	Conversion (%)		Product selectivity (%)				
	CH_4	O_2	C_2H_6	C_2H_4	C_3s	CO_2	CO
Empty[a]	30.7	69.8	6.0	13.8	1.9	8.3	70.0
Quartz chips[b]	30.5	66.9	6.3	16.0	1.8	8.1	67.9
Quartz wool[a]	33.8	76.9	5.2	15.7	1.7	8.6	68.9
Alumina[a]	28.1	78.7	6.0	17.6	1.8	8.0	66.6
SS 304[a,c]	23.4	100.0	1.1	0.6	0.0	89.9	8.4

[a] Conditions: 800°C, $D = 0.75$, CH_4/O_2 mole ratio of 2, and $Q = 50$ cc/min (at room temperature).

[b] Conditions: 800°C, $D = 0.75$, CH_4/O_2 mole ratio of 2, $Q = 33$ cc/min (at room temperature).

[c] SS, stainless steel type 304.

the activity of reactor wall materials and those used to support catalysts, the reactor was packed with quartz chips and quartz wool. Table 2 compares results from experiments using the quartz reactor empty, filled with quartz wool, and filled with quartz chips; these experiments were conducted at 800°C with feed flow rates of 50 cc/min, dilution ratios of $D = 0.75$, and methane-to-oxygen feed mole ratios of 2. The results obtained using the empty reactor and those with quartz chips at the same residence time (based on the void volume) are essentially the same indicating that quartz is relatively inert for the reaction. Results with quartz wool and with an empty alumina reactor are also similar to the empty quartz reactor results providing additional evidence that quartz does not have active sites for reaction. An empty stainless-steel reactor significantly affects methane and oxygen conversions and product selectivities. Table 2 shows that the stainless-steel reactor gave 100% oxygen conversion and yielded lower methane conversion than similar experiments using the quartz and alumina reactors. Hence, stainless steel type 304 appears to be active for total combustion and produces primarily CO_2 under these conditions.

(*g*) *Kinetics*. Power-law rate expressions were written for each of the major products and for the conversion of methane based on the feed partial pressures of methane and oxygen as shown in Table 3. Differential reaction rates were extracted from experiments in which the methane and oxygen conversions were below 10%. A multivariable linear regression fit of all the differential rates was used to obtain an empirical estimation of the rate parameters based on the power-law rate expressions and is summarized in Table 3. Figure 7 for methane conversion and Fig. 8 for ethane production compare the multivariable linear fit with a few of the differential reaction rates. Close inspection of the Arrhenius plots, Figs. 7a and 8a, reveals a deviation from linearity reflecting a more complex reaction scheme which the multivariable linear fit does not

TABLE 3

Summary of Kinetic Parameters Determined from a Multivariable Linear Fit of the Low-Conversion Results

	Preexponential factor $\mathcal{A}_i$	Activation energy E_i	Methane dependence α_i	Oxygen dependence β_i
CH_4 (conversion)	1.10×10^7	54.6	1.04	2.05
C_2H_6	3.95×10^5	51.8	1.04	1.78
C_2H_4	9.75×10^4	52.1	1.16	1.62
CO	3.23×10^{11}	71.6	0.53	3.70
CO_2	1.02×10^{-2}	29.5	−0.95	1.33

Note. $\mathcal{R}_i = \mathcal{A}_i \exp(-E_i/RT)[P_{CH_4}]^{\alpha_i}[P_{O_2}]^{\beta_i}$, where the following units are used: $\mathcal{R}_i$ (mole s^{-1}), $\mathcal{A}_i$ (mole s^{-1} (atm) $^{(\alpha+\beta)}$), E_i (kcal $mole^{-1}$), and P_i (atm).

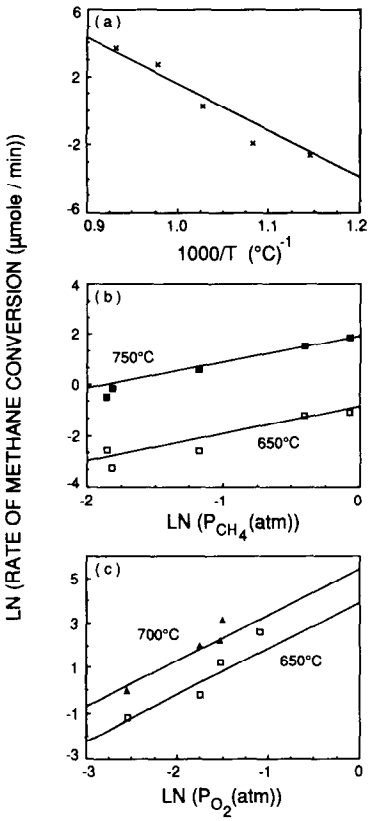

FIG. 7. (a) An Arrhenius plot for the rate of methane conversion for the low conversion data. The total feed flow rate was 50 cc/min; the dilution ratio was 0.47; the methane and oxygen partial pressures were 0.32 and 0.15 atm, respectively. (b) A power-law fit of the methane partial pressure on the rate of conversion of methane. The total feed flow rate was 50 cc/min; the temperatures were 650 and 750°C; the oxygen partial pressure was 0.08 atm. (c) A power-law fit of the oxygen partial pressure on the rate of conversion of methane. The total feed flow rate was 50 cc/min; the temperatures were 650 and 700°C; the methane partial pressure was 0.66 atm.

predict. The rates of production of C_2H_4, CO, and CO_2 are poorly fit by the power-law rate expression as reflected by the unexpected values for the dependence of methane and oxygen (see Table 3). The poor fit is not all that surprising as CO and CO_2 were observed to be secondary products in the residence time study and, thus, they do not depend on the feed partial pressures but rather on some intermediate product.

DISCUSSION

The discussion first focuses on the effects of varying the operating conditions on gas-phase conversion, product selectivity, and kinetic results with gas-phase and catalytic results being compared whenever possible. The observed results are then discussed in terms of possible gas-phase radical reaction pathways that have been presented in the combustion literature. Finally, some of the implications that these gas-phase reactions

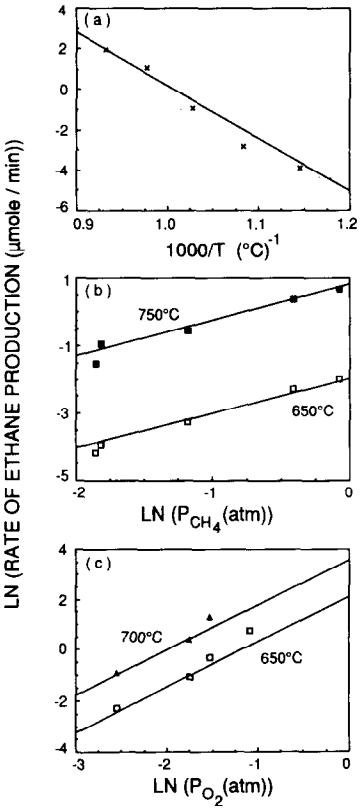

FIG. 8. (a) An Arrhenius plot for the rate of ethane production for the low conversion data. The total feed flow rate was 50 cc/min; the dilution ratio was 0.47; the methane and oxygen partial pressures were 0.32 and 0.15, respectively. (b) A power-law fit of the methane partial pressure on the rate of ethane production. The total feed flow rate was 50 cc/min; the temperatures were 650 and 750°C; the oxygen partial pressure was 0.08 atm. (c) A power-law fit of the oxygen partial pressure on the rate of ethane production. The total feed flow rate was 50 cc/min; the temperatures were 650 and 700°C; the methane partial pressure was 0.66 atm.

might have on catalytic oxidative coupling are discussed.

Operating conditions. The operating parameters were found to be critical in the gas-phase conversion of methane. The dilution ratio, oxygen partial pressure (or methane-to-oxygen mole ratio in the feed), residence time, and temperature were each found to strongly influence methane and oxygen conversions and product selectivity. The results obtained are reproducible and show conclusively that oxidative coupling occurs in the gas phase in the absence of a catalyst and independent of the reactor wall materials (if quartz or alumina is used). Table 2 shows that increasing the quartz surface area by packing the reactor with quartz chips has the same conversion as the empty quartz reactor operating at similar residence times. The empty alumina reactor, used by several groups in catalytic studies and reported to be inert (*19, 20, 40*), also gave conversions and product selectivities comparable to those obtained with the empty quartz reactors. In contrast, the stainless-steel reactor significantly affected the results indicating that it acts as a catalytic agent (refer to Table 2).

As illustrated in Figs. 2a and 2b, the partial pressure of the reactants or the degree of inert dilution significantly affects the gas-phase conversion of methane. Kimble and Kolts (*32*) have reported that little effect on product selectivity was observed in using N_2 instead of He. Since many catalytic oxidative coupling studies have fed air instead of oxygen which implies operating at relatively low reactant partial pressures, the gas-phase conversion should be relatively low. However, as shown in Table 1, not all studies have been performed at low reactant partial pressures, and in these studies there would be a contribution from gas-phase reactions.

Residence time, which can be varied by adjusting the dilution ratio, also has a significant effect on conversion and product selectivities. Figure 3 show a significant difference in conversion and selectivity resulting from changes in the residence time. An increase in residence time leads to an increase in the CO product selectivity suggesting that CO may result from the secondary combustion of ethane and/or ethylene.

Another important operating parameter for the oxidative coupling of methane is the relative partial pressures of the reactants. Increases in the oxygen partial pressure produce increases in the production of CO, and this agrees with results reported by Ito *et al.* (*29*) for lithium-promoted MgO catalysts and by Otsuka and Jinno (*43*) for Sm_2O_3 catalysts. At low oxygen partial pressures, the partial pressure of methane has only a small effect on product selectivity; however, Table 3, which includes results for higher oxygen partial pressures, shows that the feed partial pressure of methane has a positive power-law dependence on three of the major products.

Gas-phase conversions and product selectivities are compared with those reported for a LiCl/Ni oxide catalyst by Otsuka *et al.* (*39*) under one set of conditions (similar residence times) in Table 4. At high reactant partial pressures, such as is compared in Table 4 where $D = 0.7$, gas-phase reactions compete with catalytic reactions. The catalytic results, shown in Table 4, represent oxygen-limiting condi-

TABLE 4

Comparison of Gas-Phase Results with a Catalytic Study at Similar Residence Times

	Conversion (%)		Selectivity (%)	
	CH_4	O_2	C_2H_6	C_2H_4
Gas phase[a]	31.9	75.3	5.5	13.9
LiCl/Ni oxide[b]	39.4	>95.0	8.9	36.3

[a] Conditions: 750°C, $D = 0.7$, $CH_4/O_2 = 2$, and $Q = 25$ cc/min (at room temperature).

[b] Results reported by Otsuka *et al.* (*39*); conditions: 750°C, $D = 0.7$, $CH_4/O_2 = 2$, $Q = 100$ cc/min (at room temperature), and 2 g catalyst.

tions (oxygen conversion >95%) indicating that it is not appropriate to compare reaction rates with the gas-phase results with its lower oxygen conversion, 75%. Under these conditions, the methane conversion observed for the LiCl/Ni oxide catalyst is limited by the level of oxygen conversion, whereas the methane conversion observed in the gas phase is not as severely limited. Although reaction rates of catalytic results and gas-phase results cannot be directly compared, Table 4 shows that under similar conditions the gas-phase contribution can be a significant portion of the overall activity/selectivity observed in some catalytic studies. Table 4 also shows that the hydrocarbon product selectivities reported for the LiCl/Ni oxide catalyst are higher than the gas-phase values. Two points are apparent from Table 4. First, it is rather clear that the catalyst has a role in the reaction sequence and alters the product selectivity, and second, at high reactant partial pressures such as in Table 4, the gas-phase reactions are very competitive with catalytic reactions. At lower dilution ratios, the contribution from the gas phase would be less as is shown in Fig. 2 and the observed catalytic results would more accurately reflect the activity of the catalyst.

The above discussion clearly shows that the negligible gas-phase conversions reported in many catalytic studies are due to the selection of operating conditions under which the contribution from gas-phase reactions is minimal. However, as seen in Tables 1 and 4, some catalytic studies have been conducted under conditions within the range in which gas-phase reactions are contributing to the overall conversion and selectivity.

Selectivity–conversion relationships. An interesting characteristic of the observed results was that no matter which variable was changed to produce an increase in methane conversion, the product selectivities appeared to exhibit similar trends. This selectivity–conversion relationship is shown for C_2H_6, C_2H_4, CO, and CO_2 in Figs. 9a through 9d, and the experimental conditions used in obtaining these results are summarized in Table 5. Figure 9 shows that ethane selectivity decreases and CO selectivity increases when methane conversion increases. Ethylene and CO_2 product selectivities do not change as significantly with an increase in methane conversion. Figure 9 also shows that high hydrocarbon product selectivities can be achieved in the gas phase at low methane conversions which are comparable with some of the catalytic oxidative coupling studies.

TABLE 5

Experimental Conditions for Results Displayed in Fig. 9[a]

Symbol	D[b]	Q[c] (cc/min)	P_{O_2} (atm)	P_{CH_4} (atm)
⊡	0.24	50.0	0.08	0.16
◆	0.47	50.0	0.15	0.32
◘	0.70	50.0	0.23	0.47
◆	1.00	50.0	0.33	0.67
□	0.39	50.0	0.08	0.31
▲	1.00	50.0	0.08	0.92
△	0.74	50.0	0.08	0.66
■	0.84	50.0	0.18	0.66
+	0.88	50.0	0.22	0.66
⊞	0.70	13.7	0.23	0.47
×	0.70	25.0	0.23	0.47
✖	0.70	47.0	0.23	0.47
◙	0.70	102.0	0.23	0.47
■	0.70	204.0	0.23	0.47

[a] Under each of the following conditions, the results are plotted for 600, 650, 700, 750, and 800°C.
[b] $D = (P_{CH_4} + P_{O_2})/P_{TOTAL}$.
[c] Flow rate measured at room temperature.

Kinetics and reaction pathway. The reaction orders with respect to methane, determined for the power-law rate expressions by the multivariable linear fit, are first order for ethane and ethylene, one-half order for CO, and almost negative first order for CO_2 (see Table 3). Higher orders in oxygen and noninteger values obtained indicate a more complex reaction pathway and not just a simple power-law dependence on the feed partial pressures. The oxygen dependence for CO production is clearly too high and suggests that its rate of production is not

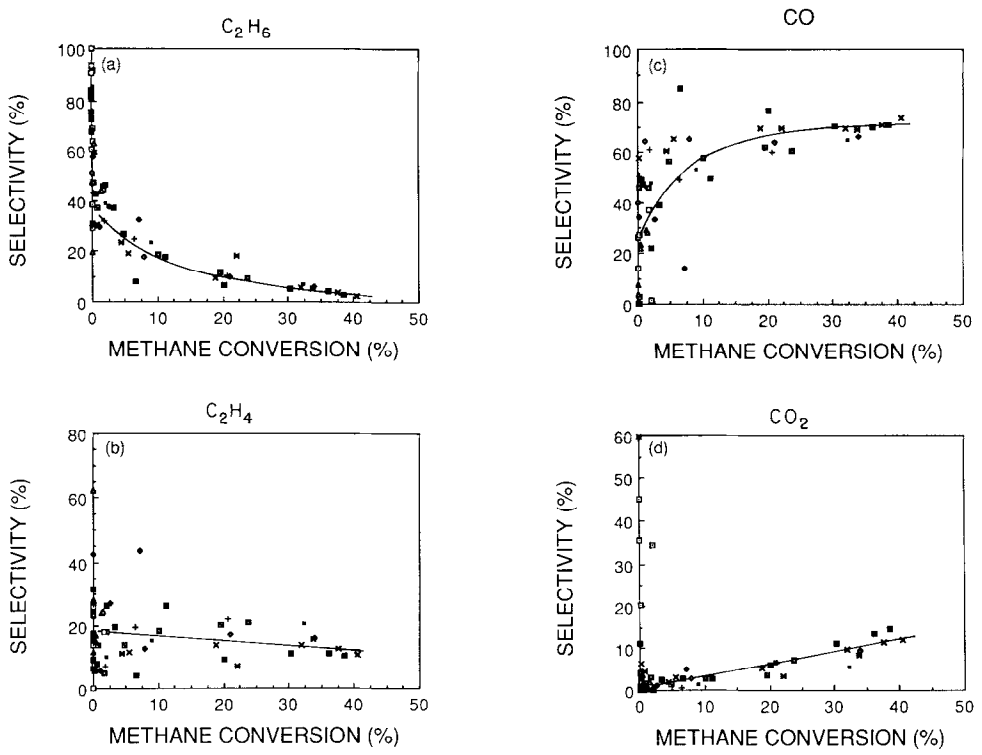

FIG. 9. Master plots showing the overall selectivity that results at varying levels of methane conversions independent of the operating conditions. The resulting product selectivities are shown for C_2H_6, C_2H_4, CO, and CO_2 as a function of methane conversion in (a, b, c, and d), respectively. The experimental conditions for each set of results are summarized in Table 5.

dependent on the partial pressure of the feed reactants but rather on an intermediate product.

The apparent activation energies, shown in Table 3, for the conversion of methane and the production of ethane and ethylene are approximately the same with an average of about 53 kcal/mole. This indicates that the same reaction pathway or at least the same rate-limiting step may be involved; most likely this step is the abstraction of the first hydrogen from methane. These apparent activation energies agree fairly well with others reported by catalytic studies for C_2 hydrocarbon formation. Ito *et al.* (*29*) have reported an apparent activation energy of 55.2 kcal/mole for Li-promoted MgO catalysts, Labinger and Ott (*20*) have reported a value of 58 kcal/mole for a Mn–Mg oxide catalyst, and Asami *et al.* (*45*) have reported a value of 50.3 kcal/mole for a PbO/MgO catalyst. In addition, these values are similar to those reported for the formation of methyl radicals formed by the gas-phase reaction of methane and molecular oxygen:

$$CH_4 + [O_2] \rightarrow CH_3\cdot + HO_2\cdot \qquad (1)$$

The activation energy for the above reaction has been reported to be 57.28 and 56.00 kcal/mole by Tsang and Hampson (*53*) and Skinner *et al.* (*54*), respectively. It appears that the rate-limiting step in both the gas-phase study reported here and the catalytic studies reported elsewhere (*20, 29, 45*) have essentially the same apparent activation energies around 55 kcal/mole. The observed rates of ethane and ethylene production increase as temperature increases, but the product selectivities are lower because

TABLE 6

Possible Gas-Phase Radical Reactions

Primary mode of initiation	$CH_4 + [O_2] \rightarrow CH_3\cdot + HO_2\cdot$	(1)
Chain propagation	$CH_4 + HO_2\cdot \rightarrow CH_3\cdot + H_2O_2$	(2)
	$CH_4 + \cdot OH \rightarrow CH_3\cdot + H_2O$	(3)
Secondary chain initiation	$H_2O_2 + Z \rightarrow 2\ \cdot OH + Z$	(4)
	where Z is a third body	
Ethane formation by methyl radical termination	$CH_3\cdot + CH_3\cdot \rightarrow C_2H_6$	(5)
Ethylene formation		
Thermally	$C_2H_6 \rightarrow C_2H_4 + H_2$	(6)
Radical branching and chain transfer	$C_2H_6 + [O_2] \rightarrow C_2H_5\cdot + HO_2\cdot$	(7)
	$C_2H_6 + Y\cdot \rightarrow C_2H_5\cdot + HY$	(8)
	$C_2H_5\cdot + [O_2] \rightarrow C_2H_4 + HO_2\cdot$	(9)
	where $Y\cdot$ is $CH_3\cdot$, $HO_2\cdot$, or $\cdot OH$ radicals	
Oxidation product formation	$CH_3\cdot + [O_2] \rightarrow CH_3O_2\cdot$	(10)
	$CH_3O_2\cdot \rightarrow CH_2O + \cdot OH$	(11)
	$CH_2O + [O_2] \rightarrow CHO\cdot + HO_2\cdot$	(12)
	$CH_2O + X\cdot \rightarrow CHO\cdot + XH$	(13)
	$CHO\cdot + [O_2] \rightarrow CO + HO_2\cdot$	(14)
	where $X\cdot$ could be any radical	
Secondary combustion	$C_2H_6 + [O_2] \rightarrow CO, CO_2$	(15)
	$C_2H_4 + [O_2] \rightarrow CO, CO_2$	(16)
	$CO + [O_2] \rightarrow CO_2$	(17)
Termination reactions	$HO_2\cdot + HO_2\cdot \rightarrow H_2O_2 + O_2$	(18)
	$H_2O_2 \rightarrow H_2O + \frac{1}{2}O_2$	(19)

the production of CO increases significantly when the temperature is raised. This implies that the apparent activation energy for CO production is larger than those for hydrocarbon production which agrees with the value obtained from the lumped-kinetic results (Table 3).

The observed gas-phase results can be used to consider several possible reactions that participate in the reaction pathway leading to the various products. In writing the reactions involving oxygen, the oxygen species is represented in square brackets to indicate that it represents gas-phase molecular oxygen in this work; however, in the catalytic studies, it is probably *both* gas-phase and surface or lattice oxygen. Once the formation of radicals has been initiated, many reactions are known to be important (*53*). Only a few of the major reactions are considered here and all are based on reaction networks already reported in the literature for combustion reactions.

Geisbrecht and Daubert (*55*) have considered a series of reactions similar to reactions (1) through (4) for the vapor-phase oxidation of ethane. These four reactions, shown in Table 6, seem to be likely candidates for the radical initiation and chain propagation reactions that occur during the gas-phase oxidative coupling of methane. As previously mentioned, the apparent activation energy for methane conversion found in this work is similar to that reported for reaction (1). Although several catalytic studies have indicated that the rate-limiting step is the formation of methyl radicals (*19, 29, 30, 32*), the importance of reaction (1) in the gas phase is the formation of hydroperoxy radicals, $HO_2\cdot$. This is supported by the fact that the rate of methane conversion observed in this study at 800°C is about four orders of magnitude higher than the predicted rate of reaction (1) for methyl radical production based on gas-phase literature values (*53*). The $HO_2\cdot$ radicals, generated by reaction (1), can then undergo chain propagation via reaction (2)

similar to the reaction mechanism proposed by Geisbrecht and Daubert for ethane (*55*). Tsang and Hampson (*53*) have reported that reaction (2) proceeds at an extremely fast rate under these conditions with a rate constant of $3.0 \times 10^{-13} \exp(-9350/T)$ (cm^3 $molecule^{-1}$ s^{-1}). Although $HO_2\cdot$ radicals have not been reported in other studies, the $HO_2\cdot$ radical concentration would only have to be about 30 molecules/cm^3 in order for reaction (2) to proceed at a fast enough rate to produce enough methyl radicals for the methane conversion observed in this study.

In addition, reaction rates predicted from literature values suggest that the hydroxyl radical might also be participating in a chain propagation step producing additional methyl radicals through reaction (3). Hydroxyl radicals can be produced through a secondary chain initiation step by the decomposition of hydrogen peroxide shown in reaction (4). Since the rates of the chain propagation steps, reactions (2) and (3), have much higher reaction rate constants than reaction (1), the majority of the methyl radicals are thought to be generated through chain propagation.

Similar to catalytic oxidative coupling reaction pathways (*20, 21, 29, 32, 33*), the methyl radicals generated through initiation and chain propagation are assumed to recombine forming ethane by reaction (5). Using matrix isolation–electron spin resonance (MIESR) techniques with a probe, Campbell *et al.* (*56*) have reported that methyl radicals are detected in the gas phase and that at least 40% of the ethane formation takes place in the gas phase. Literature values (*53, 54*) for the gas-phase rate constant of reaction (5), shown in Table 6, are around 1.16×10^{13} cm^3 $mole^{-1}$ s^{-1} or 1.93×10^{-11} cm^3 $molecule^{-1}$ s^{-1}. Other studies have indicated that both thermal and oxidative dehydrogenations contribute to ethylene production (*18, 20, 21*). Since the activation energy for the formation of ethylene from ethane has been reported to be less than 10 kcal/mole (*33*), it is not surprising that the apparent activation energies for ethane and ethylene production are similar (refer to Table 3). Once ethane has been formed by reaction (5), it has been reported to undergo thermal dehydrogenation to ethylene via reaction (6) and oxidative dehydrogenation via the secondary chain initiation, reaction (7). Radical branching and chain transfer reactions might also participate in dehydrogenating ethane, reaction (8), which would produce ethyl radicals, $C_2H_5\cdot$. The ethyl radicals are then readily oxidized by reaction (9). The relative importance of each reaction rate for Eqs. [6] to [9], shown in Table 6, is not clear but is currently under investigation.

The reaction pathway for the formation of the oxidation products is not entirely clear. Numerous reactions are known to occur in the combustion of methane (*53*). Among these reactions, reactions (10) through (14) shown in Table 6 are considered relevant to this study. The formation of $CH_3O_2\cdot$ radicals, produced by reaction (10), has been observed by Driscoll *et al.* (*57*) at relatively high oxygen partial pressures using MIESR techniques. In addition, the $CH_3O_2\cdot$ radicals are considered to be intermediates in the combustion of methane (*29, 58*). In a reaction scheme similar to that used in methane combustion (*58–60*), the methylperoxy radicals can further react to form CO via reactions (12) through (14). These reaction steps are supported by the detection of trace amounts of formaldehyde (dissolved in the water trapped at the reactor exit) which is a product of reaction (11). Raising the methane partial pressure and lowering the oxygen partial pressure would decrease the production of $CH_3O_2\cdot$ radicals and presumably decrease CO production which is consistent with what is shown in Figs. 4 and 5.

In this study, longer residence times gave higher rates of CO production and lower hydrocarbon product selectivities suggesting that the desired products are being combusted. Carbon monoxide also appears to result from the secondary oxidation of ethane and ethylene shown by reactions (15)

and (16) (Table 6) which omit several intermediate steps. By comparison of the bond dissociation energies of the first C–H bond for ethane (98 kcal/mole) and ethylene (104 kcal/mole) with those of methane (104 kcal/mole) (*1*), it is apparent that when operating conditions are sufficient for methyl radical formation they are also adequate for causing the destruction of the desired products. The formation of CO and CO_2 from C_2 hydrocarbons has been identified in catalytic studies (*18, 20, 21, 24*). Although in catalytic studies CO_2 has been reported to be the primary oxidation product, CO was the major oxidation product observed in this work. This indicates that the catalyst in catalytic oxidative coupling may be activating the complete combustion of hydrocarbons to CO_2. Carbon dioxide also appears to result from the oxidation of CO in the gas phase by reaction (16). This was based on experiments in which CO and O_2 were cofed to the reactor under operating conditions similar to those used in oxidative coupling studies.

Two of the termination reactions that are reported for methane combustion (*60*) and ethane combustion (*55*) are shown in reactions (18) and (19) in Table 6. Hydroperoxy radicals, $HO_2\cdot$, are reported to terminate by reaction (18), and methyl radicals, $CH_3\cdot$, terminate by producing ethane by reaction (5). Termination steps are often neglected for the hydroxyl radicals due to their high reactivity and have not been considered. In addition, hydrogen peroxide, H_2O_2, can decompose by reaction (19) instead of reaction (4) which, in a sense, represents a termination step since hydroxyl radicals are not generated.

The higher hydrocarbons, primarily propylene, were formed at high methyl radical and ethylene concentrations. Similar to the reaction pathways proposed by Kimble and Kolts (*32*) and by Labinger and Ott (*20*), the higher hydrocarbons are probably formed by degenerate branching and chain transfer reactions between methyl and ethyl radicals. These reactions have not been included since the production of the higher hydrocarbons was relatively small compared to that of ethane and ethylene.

Although the reaction steps presented in Table 6 are consistent with combustion studies and the experimental results presented here, the overall reaction pathway is probably more complex. It should be emphasized that these steps are speculative and were intended to give a qualitative understanding of some of the chemistry involved.

Implications for catalytic studies. This study of gas-phase reactions during the oxidative coupling of methane suggests that a new perspective on the role of gas-phase reactions should be considered. No methane decomposition was observed in this gas-phase study in the absence of oxygen; however, when methane and oxygen were cofed, hydrocarbon product selectivities of 29% were observed at a methane conversion of 32%. Otsuka *et al.* (*61*) studying catalytic oxidative coupling have suggested that "the active oxygen species capable to break (the first) C–H bond of CH_4 can not be created from the oxygen in the gas phase." Clearly the results presented herein suggest that such evidence is not so definitive.

After submitting this paper, two communications recently appeared in the literature which report that gas-phase reactions are important at elevated pressures (*62, 63*). These studies confirm that gas-phase reactions need to be understood and can contribute to some of the observed activity in catalytic studies under some operating conditions. In addition, there are several parallels between the effects of increasing the pressure in the elevated pressure study and increasing the partial pressure of the reactants shown in Figs. 2a and 2b.

Beyond showing that oxidative coupling can occur in the gas phase, several important points are indicated by this study. The role that the catalyst plays is not well understood in catalytic oxidative coupling. This gas-phase study indicates that perhaps

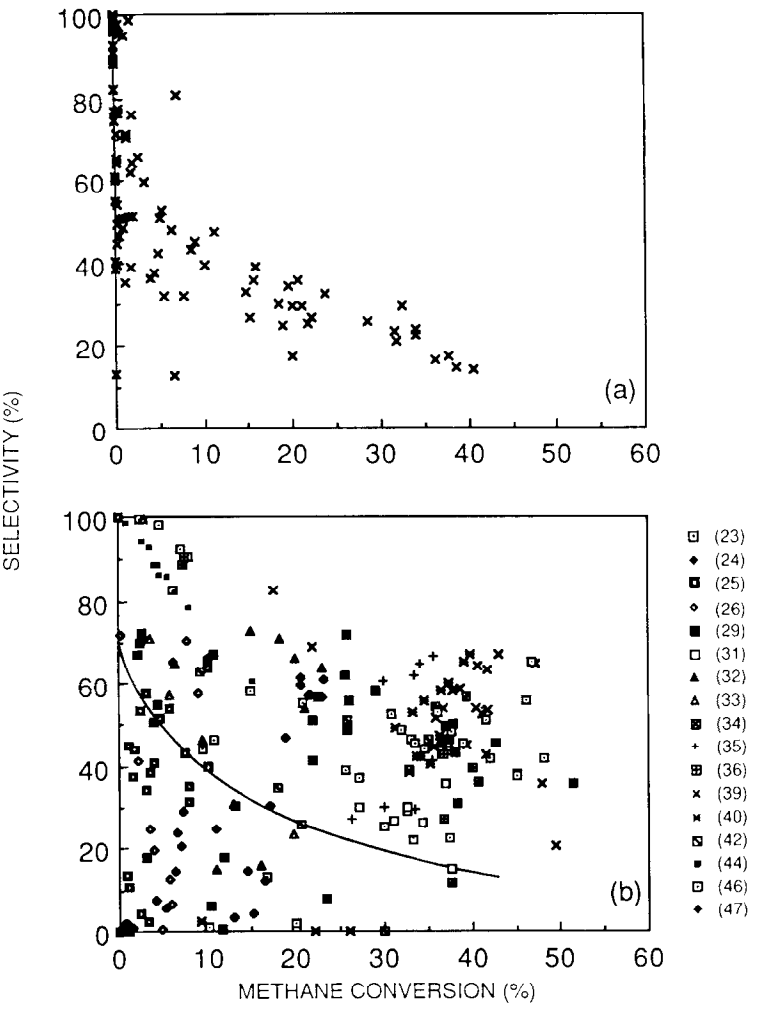

FIG. 10. Comparison of hydrocarbon product selectivities at different methane conversions. (a) Results obtained in this gas-phase study. (b) Results reported in the literature by various authors as cited in the legend. The line represents a visual fit of the noncatalytic, gas-phase results shown in (a).

the role of the catalyst is to increase the local oxygen concentration and thus increase the probability of hydrogen abstraction from methane. This is similar to raising the oxygen partial pressure in gas-phase reaction experiments. After methyl radicals are formed, as shown by Lunsford and coworkers (*29, 56*), the catalyst can then alter the product selectivity depending on its oxygen surface chemistry. In addition, if the hydrocarbon-forming chemistry takes place exclusively in the gas phase (*18, 20, 21, 32*), the role of a "good" oxidative coupling catalyst becomes the minimization of CO and CO_2 production from the sequential combustion of the desired products. This is probably part of the reason that low surface area catalysts and alkali promotion of catalysts have been reported to have relatively high hydrocarbon yields (*18, 31*). Several studies have suggested that the catalyst abstracts a hydrogen from methane and the hydrocarbon-forming chemistry takes place in the gas phase (*32, 56*).

Figures 9a through 9d indicate that the product selectivities resulting from gas-

phase reactions follow a general trend independent of which operating parameter was changed to increase the methane conversion. These trends appear to be limiting values for product selectivities at high conversions. However, some of the catalytic oxidative coupling studies have reported values better than the trends shown in Fig. 9. Figures 10a and 10b compare the hydrocarbon product selectivity at various methane conversions for the gas-phase results and for some results reported in the literature, respectively. It is apparent from Fig. 10b that the catalyst has changed the product selectivity and has altered the radical reaction pathway; however, sufficiently high yields have yet to be reported at steady state.

SUMMARY

Depending on operating conditions, the gas-phase reaction of methane and oxygen can produce significant conversions to ethane and ethylene. The results suggest that some of the conditions used in catalytic oxidative coupling which have been reported in the literature are in the range of conditions under which gas-phase kinetics are affecting the catalytic results. Gas-phase oxidative coupling can be minimized by operating at low reactant partial pressures, low oxygen partial pressures (high CH_4/O_2 feed ratios), and short residence times. Since the reactions occurred in the gas phase, variations in reactor design can also be used to alter the contribution of the gas-phase kinetics.

A survey of operating conditions was used to estimate lumped kinetic parameters. The apparent activation energies for the conversion of methane and the production of ethane and ethylene are around 53 kcal/mole. The apparent activation energy for methane conversion is similar to that reported for the gas-phase reaction of methane and oxygen as

$$CH_4 + O_2 \rightarrow CH_3\cdot + HO_2\cdot$$

Thus, the above reaction could possibly be the rate-limiting step and the primary mode of radical initiation. A reaction pathway is considered in which the hydroperoxy radicals, $HO_2\cdot$, produced by the above reaction, and hydroxyl radicals generate methyl radicals by chain propagation. Once the methyl radicals have been generated, hydrocarbon-forming chemistry can take place by radical reactions in the gas phase. Ethane is most likely formed by the recombination of methyl radicals, and ethylene is probably formed by a combination of oxidative and radical dehydrogenation of ethane. Carbon monoxide and to a lesser extent CO_2 are considered to be produced from the oxidation of methyl radicals and the combustion of ethane and ethylene.

ACKNOWLEDGMENT

The authors gratefully acknowledge the Amoco Research Center, Naperville, Illinois, for providing financial support for this work.

REFERENCES

1. Kerr, J. A., *Chem. Rev.* **66,** 465 (1966).
2. Keller, G. E., and Bhasin, M. M., *J. Catal.* **73,** 9 (1982).
3. Pitchai, R., and Klier, K., *Catal. Rev. Sci. Eng.* **28,** 13 (1986).
4. Chamberlin, D. S., and Bloom, E. B., *Ind. Eng. Chem.* **21,** 945 (1929).
5. Happel, J., and Kramer, L., *Ind. Eng. Chem.* **59,** 39 (1967).
6. Van Hook, J. P., *Catal. Rev. Sci. Eng.* **21,** 1 (1980).
7. Bartholomew, C. H., *Catal. Rev. Sci. Eng.* **24,** 67 (1982).
8. Scurrell, M. S., *Appl. Catal.* **32,** 1 (1987).
9. Anderson, J. R., and Tsai, P., *Appl. Catal.* **19,** 141 (1985).
10. Khan, M. M., and Somorjai, G. A., *J. Catal.* **91,** 263 (1985).
11. Liu, R.-S., Iwamoto, M., and Lunsford, J. H., *J. Amer. Chem. Soc. Commun.* **78,** 78 (1982).
12. Liu, H.-F., Liu, R.-S., Liew, K. Y., Johnson, R. E., and Lunsford, J. H., *J. Amer. Chem. Soc.* **106,** 4117 (1984).
13. Meng, H., and Sanger, A. R., *Appl. Catal.* **32,** 347 (1987).
14. Otsuka, K., and Nakajima, T., *J. Chem. Soc. Faraday Trans. 1* **83,** 1315 (1987).
15. Solymosi, F., Tombacz, I., and Kutsan, G., *J. Chem. Soc. Chem. Commun.,* 1455 (1985).
16. Zhen, K. J., Khan, M. M., Mak, C. H., Lewis, K. B., and Somorjai, G. A., *J. Catal.* **94,** 501 (1985).

17. Gesser, H. D., Hunter, N. R., and Prakash, C. B., *Chem. Rev.* **85,** 235 (1985).
18. Jones, C. A., Leonard, J. J., and Sofranko, J. A., *J. Catal.* **103,** 311 (1987).
19. Labinger, J. A., Ott, K. C., Mehta, S., Rockstad, H. K., and Zoumalan, S., *J. Chem. Soc. Chem. Commun.*, 543 (1987).
20. Labinger, J. A., and Ott, K. C., *J. Phys. Chem.* **91,** 2682 (1987).
21. Sofranko, J. A., Leonard, J. J., and Jones, C. A., *J. Catal.* **103,** 302 (1987).
22. Mars, P., and van Krevelen, D. W., *Chem. Eng. Sci. Suppl.* **3,** 41 (1954).
23. Aika, K.-I., Moriyama, T., Takasaki, N., and Iwamatsu, E., *J. Chem. Soc. Chem. Commun.*, 1210 (1986).
24. Ali Emesh, I. T., and Amenomiya, Y., *J. Phys. Chem.* **90,** 4785 (1986).
25. Asami, K., Hashimoto, S., Shikada, T., Fujimoto, K., and Tominaga, H.-O., *Chem. Lett.*, 1233 (1986).
26. Bytyn, W., and Baerns, M., *Appl. Catal.* **28,** 199 (1986).
27. Hinsen, W., Bytyn, W., and Baerns, M., "Proceedings, 8th International Congress on Catalysis, Berlin, 1984," Vol. III, p. 581. Dechema, Frankfurt-am-Main, 1984.
28. Imai, H., and Tagawa, T., *J. Chem. Soc. Chem. Commun.*, 52 (1986).
29. Ito, T., Wang, J.-X., Lin, C.-H., and Lunsford, J. H., *J. Amer. Chem. Soc.* **107,** 5062 (1985).
30. Ito, T., and Lunsford, J. H., *Nature (London)* **314,** 721 (1985).
31. Iwamatsu, E., Moriyama, T., Takasaki, N., and Aika, K.-I., *J. Chem. Soc. Chem. Commun.* **19** (1987).
32. Kimble, J. B., and Kolts, J. H., *Energy Prog.* **6,** 226 (1986).
33. Lin, C.-H., Campbell, K. D., Wang, J.-X., and Lunsford, J. H., *J. Phys. Chem.* **90,** 534 (1986).
34. Lin, C.-H., Ito, T., Wang, J.-X., and Lunsford, J. H., *J. Amer. Chem. Soc.* **109,** 4808 (1987).
35. Matsuura, I., Utsumi, Y., Nakai, M., and Doi, T., *Chem. Lett.*, 1981 (1986).
36. Moriyama, T., Takasaki, N., Iwamatsu, E., and Aika, K.-I., *Chem. Lett.*, 1165 (1986).
37. Otsuka, K., Jinno, K., and Morikawa, A., *Chem. Lett.*, 499 (1985).
38. Otsuka, K., Liu, Q., Hatano, M., and Morikawa, A., *Chem. Lett.*, 467 (1986).
39. Otsuka, K., Liu, Q., Hatano, M., and Morikawa, A., *Chem. Lett.*, 903 (1986).
40. Otsuka, K., and Komatsu, T., *Chem. Lett.*, 1955 (1986).
41. Otsuka, K., and Komatsu, T., *Chem. Lett.*, 483 (1987).
42. Otsuka, K., Liu, Q., and Morikawa, A., *Inorg. Chim. Acta* **118,** L23 (1986).
43. Otsuka, K., and Jinno, K., *Inorg. Chim. Acta* **121,** 237 (1986).
44. Otsuka, K., Jinno, K., and Morikawa, A., *J. Catal.* **100,** 353 (1986).
45. Asami, K., Shikada, T., Fujimoto, K., and Tominaga, H.-O., *Ind. Eng. Chem. Res.* **26,** 2348 (1986).
46. Otsuka, K., and Komatsu, T., *J. Chem. Soc. Chem. Commun.*, 388 (1987).
47. Yamagata, N., Tanaka, S. S., Sasaki, S., and Okazaki, S., *Chem. Lett.* **81** (1987).
48. Burgess, M. J., and Wheeler, R. V., *J. Chem. Soc. Trans.* **105,** 2596 (1914).
49. Cooper, C. M., and Wiezevich, P. J., *Ind. Eng. Chem.* **21,** 1210 (1929).
50. Mason, W., and Wheeler, R. V., *J. Chem. Soc.* **113,** 47 (1918).
51. White, A. G., *J. Chem. Soc. Trans.* **127,** 672 (1925).
52. Shtern, V. Ya., "The Gas-Phase Oxidation of Hydrocarbons," Chap. 7, pp. 387–436. Macmillan Co., New York, 1964.
53. Tsang, W., and Hampson, R. F., *J. Phys. Chem. Ref. Data* **15,** 1087 (1986).
54. Skinner, G. B., Lifshitz, A. V., Scheller, K., and Burcat, A., *J. Chem. Phys.* **56,** 3853 (1972).
55. Geisbrecht, R. A., and Daubert, T. E., *Ind. Eng. Chem. Process Des. Dev.* **14,** 159 (1975).
56. Campbell, K. D., Morales, E., and Lunsford, J. H., *J. Amer. Chem. Soc.* **109,** 7900 (1987).
57. Driscoll, D. J., Martir, W., Wang, J.-X., and Lunsford, J. H., *J. Amer. Chem. Soc.* **107,** 58 (1985).
58. Boudart, M., "Kinetics of Chemical Processes." Prentice–Hall, Englewood Cliffs, NJ, 1968.
59. Selby, K., and Waddington, D. J., *J. Chem. Soc. Perkin Trans. II,* 1259 (1979).
60. Benson, S. W., and Nangia, P. S., *Acc. Chem. Res.* **12,** 223 (1979).
61. Otsuka, K., Said, A. A., Jinno, K., and Komatsu, T., *Chem. Lett.*, 77 (1987).
62. Asami, K., Omata, F., Fujimoto, K., and Tominaga, H.-O., *J. Chem. Soc. Chem. Commun.*, 1287 (1987).
63. Hutchings, G. J., Scurrell, M. S., and Woodhouse, J. R., *J. Chem. Soc. Chem. Commun.*, 253 (1988).